

# WASP-30b: A 61 $M_{\text{Jup}}$ BROWN DWARF TRANSITING A $V=12$ , F8 STAR

D. R. ANDERSON<sup>1</sup>, A. COLLIER CAMERON<sup>2</sup>, C. HELLIER<sup>1</sup>, M. LENDL<sup>3</sup>, P. F. L. MAXTED<sup>1</sup>, D. POLLACCO<sup>4</sup>, D. QUELOZ<sup>3</sup>,  
 B. SMALLEY<sup>1</sup>, A. M. S. SMITH<sup>1</sup>, I. TODD<sup>4</sup>, A. H. M. J. TRIAUD<sup>3</sup>, R. G. WEST<sup>5</sup>, S. C. C. BARROS<sup>4</sup>, B. ENOCH<sup>2</sup>,  
 M. GILLON<sup>6</sup>, T. A. LISTER<sup>7</sup>, F. PEPE<sup>3</sup>, D. SÉGRANSAN<sup>3</sup>, R. A. STREET<sup>7</sup>, S. UDRY<sup>3</sup>

*Draft version December 6, 2010*

## ABSTRACT

We report the discovery of a 61-Jupiter-mass brown dwarf, which transits its F8V host star, WASP-30, every 4.16 days. From a range of age indicators we estimate the system age to be 1–2 Gyr. We derive a radius ( $0.89 \pm 0.02 R_{\text{Jup}}$ ) for the companion that is consistent with that predicted ( $0.914 R_{\text{Jup}}$ ) by a model of a 1-Gyr-old, non-irradiated brown dwarf with a dusty atmosphere. The location of WASP-30b in the minimum of the mass-radius relation is consistent with the quantitative prediction of Chabrier & Baraffe (2000), thus confirming the theory.

*Subject headings:* binaries: eclipsing — stars: low-mass, brown dwarfs — stars: individual (WASP-30)

## 1. INTRODUCTION

A brown dwarf (BD) is traditionally defined as an object with a mass above the deuterium-burning limit ( $13 M_{\text{Jup}}$ ; e.g. Chabrier et al. 2000a) and below the hydrogen-burning limit ( $0.07 M_{\odot}$ ; e.g. Chabrier et al. 2000b). However, an alternative suggestion is that the manner in which an object forms should determine whether it is a planet or a BD. Thus, if an object formed by core accretion of dust and ices in a protoplanetary disc then it would be a planet, and if it formed by gravoturbulent collapse of a molecular cloud, as do stars, then it would be a BD.

Studies such as the Caballero et al. (2007) observations of a young open cluster core find a continuous mass function down to  $\sim 6 M_{\text{Jup}}$ , indicating that the star formation mechanism can produce objects with planetary masses. This is supported by theoretical studies (Padoan & Nordlund 2004; Hennebelle & Chabrier 2008) which suggest that gravoturbulent fragmentation of molecular clouds produces stars and BDs down to a few Jupiter masses in numbers comparable to the observationally-determined distribution. In contrast, when taking into account planetary migration through the protoplanetary disc, the core accretion process might result in giant planets with masses of up to  $10 M_{\text{Jup}}$  (Alibert et al. 2005), or even  $25 M_{\text{Jup}}$  (Mordasini et al. 2008). Sahlmann et al. (2010) see evidence for a bimodal distribution in brown dwarf masses, with the less-massive group presumably representing the high-mass

tail of the planetary distribution.

An accurate, precise measurement of an object's radius is therefore required to probe for the existence of a core and thus discriminate between the two formation mechanisms. For example, the radius of the  $8-M_{\text{Jup}}$  body, HAT-P-2b, is consistent with an irradiated planet incorporating a 340-Earth-mass core, but is smaller than if it were coreless (Leconte et al. 2009). The  $22-M_{\text{Jup}}$  CoRoT-3b (Deleuil et al. 2008) is sufficiently massive to qualify as a BD under the traditional definition, but the radius of this object is uncertain at the 7% level. This is higher than the 3% required to discriminate between the absence or presence of a core and thus determine how it formed (Leconte et al. 2009). Irwin et al. (2010) found a  $\sim 30-M_{\text{Jup}}$  BD, NLTT 41135C, which transits one member of an M-dwarf binary system. However, as the transits are grazing, it is not currently possible to accurately measure its radius.

There is less ambiguity around the upper end of the BD mass regime: if a body is sufficiently massive to fuse hydrogen then it is a star, otherwise it is a BD. High-mass BDs with precise radius measurements are useful for testing BD evolution models, as it is in the high-mass regime that models predict the greatest changes in radius with age (e.g. Baraffe et al. 2003). Stassun et al. (2006) discovered a BD eclipsing binary system in the Orion Nebula star-forming region, with masses of  $57 \pm 5 M_{\text{Jup}}$  and  $36 \pm 3 M_{\text{Jup}}$ . With very large radii of  $0.699 \pm 0.034 R_{\odot}$  and  $0.511 \pm 0.026 R_{\odot}$ , it seems that these objects are in the earliest stages of gravitational contraction. Similar to the NLTT 41135 system, LHS 6343 C (Johnson et al. 2010, Johnson 2010, private communication) is a  $63-M_{\text{Jup}}$  BD that transits one member of an M-dwarf binary system. In this case, the transits are full and so the radius ( $0.825 \pm 0.023 R_{\text{Jup}}$ ) of this object is precisely determined. CoRoT-15b (Bouchy et al. 2010) is a  $63-M_{\text{Jup}}$ -mass BD in a 3-d orbit around an F7V star. Due to the faintness of the host star ( $V \sim 16$ ), the BD radius ( $1.12^{+0.30}_{-0.15} R_{\text{Jup}}$ ) is not yet well determined.

To test and refine models of BD formation and evolution, a population of well-characterised objects is required. In this letter, we present the discovery of WASP-30b, a  $61-M_{\text{Jup}}$  brown dwarf that transits its moderately-

dra@astro.keele.ac.uk

<sup>1</sup> Astrophysics Group, Keele University, Staffordshire, ST5 5BG, UK

<sup>2</sup> SUPA, School of Physics and Astronomy, University of St. Andrews, North Haugh, Fife, KY16 9SS, UK

<sup>3</sup> Observatoire de Genève, Université de Genève, 51 Chemin des Maillettes, 1290 Sauverny, Switzerland

<sup>4</sup> Astrophysics Research Centre, School of Mathematics & Physics, Queen's University, University Road, Belfast, BT7 1NN, UK

<sup>5</sup> Department of Physics and Astronomy, University of Leicester, Leicester, LE1 7RH, UK

<sup>6</sup> Institut d'Astrophysique et de Géophysique, Université de Liège, Allée du 6 Août, 17, Bat. B5C, Liège 1, Belgium

<sup>7</sup> Las Cumbres Observatory, 6740 Cortona Dr. Suite 102, Santa Barbara, CA 93117, USA

TABLE 1  
RADIAL VELOCITY MEASUREMENTS OF WASP-30

BJD-2 450 000 (days)	RV (km s <sup>-1</sup> )	$\sigma_{RV}$ (km s <sup>-1</sup> )	BS (km s <sup>-1</sup> )
5009.9065	14.275	0.032	0.077
5040.8722	1.298	0.050	-0.190
5092.6977	14.348	0.044	0.048
5095.6894	5.163	0.030	-0.039
5096.5476	12.979	0.040	-0.020
5096.8712	14.452	0.041	0.005
5097.5351	12.509	0.041	0.052
5097.8735	9.732	0.048	0.039
5098.5538	3.350	0.040	-0.006
5113.5209	14.451	0.031	-0.127
5113.5877	14.563	0.036	-0.008
5113.6111	14.515	0.038	-0.009
5113.6343	14.582	0.034	-0.094
5113.6576	14.488	0.031	-0.032
5113.6809	14.535	0.030	-0.059
5113.7041	14.508	0.031	-0.061

bright host star.

## 2. OBSERVATIONS

WASP-30 is a  $V = 11.9$ , F8V star located in Aquarius, on the border with Cetus. A transit search (Collier Cameron et al. 2006) of WASP-South data from 2008 July to November found a strong, 4.16-d periodicity. Further observations in 2009 with both WASP instruments (Pollacco et al. 2006) led to a total of 17612 usable photometric measurements (Figure 1).

Using the CORALIE spectrograph mounted on the 1.2-m Euler-Swiss telescope (Baranne et al. 1996; Queloz et al. 2000), we obtained 16 spectra of WASP-30 in 2009. Radial velocity (RV) measurements were computed by weighted cross-correlation (Baranne et al. 1996; Pepe et al. 2005) with a numerical G2-spectral template. RV variations were detected with the same period found from the WASP photometry and with a semi-amplitude of  $6.6 \text{ km s}^{-1}$ , consistent with a sub-stellar-mass companion. The RV measurements are listed in Table 1 and are plotted in Figure 1.

To test the hypothesis that the RV variations are due to spectral line distortions caused by a blended eclipsing binary or starspots, we performed a line-bisector analysis (Queloz et al. 2001) of the CORALIE cross-correlation functions. The lack of correlation between bisector span and RV (Figure 1) supports our conclusion that the periodic dimming of WASP-30 and its RV variations are due to the sub-stellar orbiting body, WASP-30b.

To refine the system parameters, we obtained high signal-to-noise transit photometry through a Gunn  $r$  filter with the Euler-Swiss telescope on 2010 Aug 01 (Figure 1; Table 2). The data were affected by light cloud and a guiding issue caused by the close proximity of the bright Moon (69% illumination,  $26^\circ$  from target).

## 3. STELLAR PARAMETERS

The 16 CORALIE spectra of WASP-30 were co-added to produce a single spectrum with a typical S/N of around 70:1. The analysis was performed using the methods given in Gillon et al. (2009). The  $H_\alpha$  line was used to determine the effective temperature ( $T_{\text{eff}}$ ), while the Na I D and Mg I b lines were used as surface gravity ( $\log g_*$ )

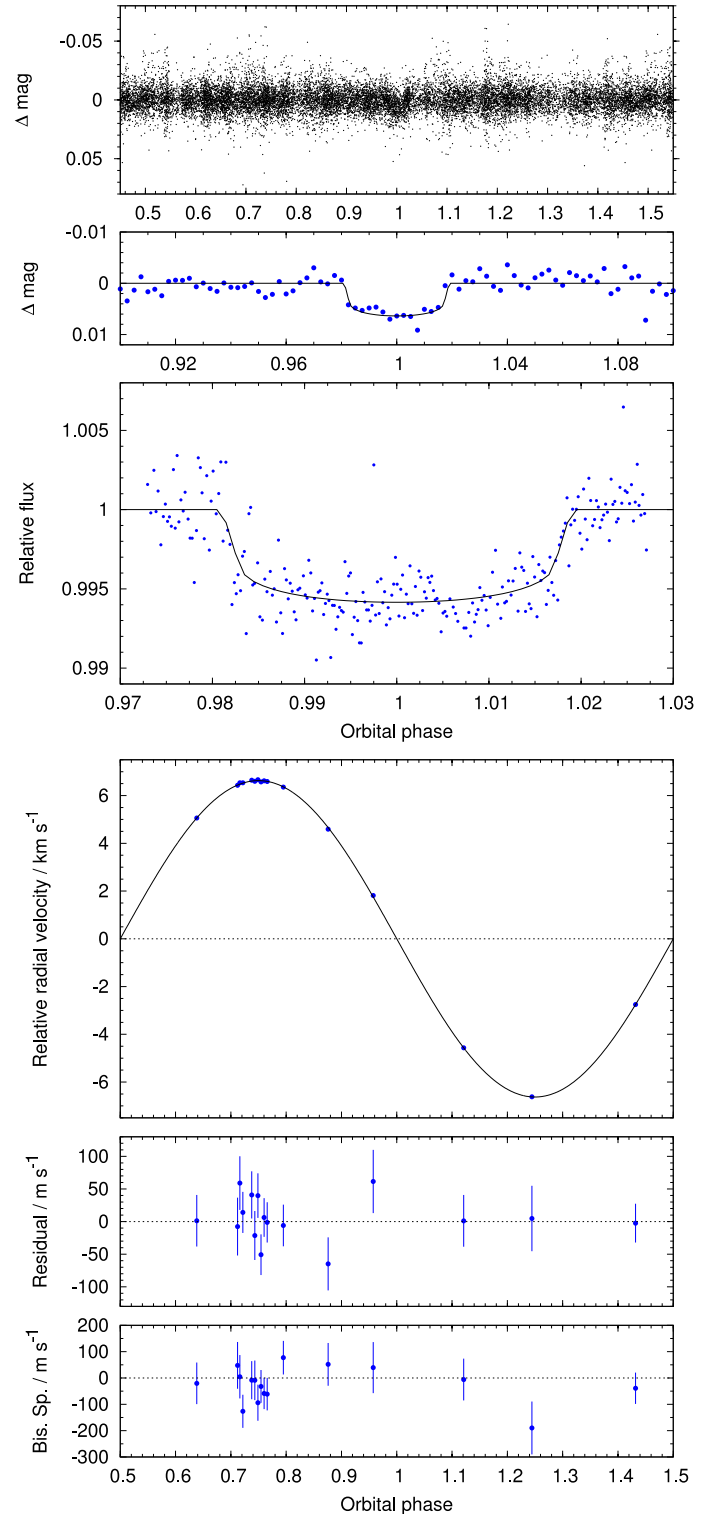


FIG. 1.— **Top panel:** WASP discovery light curve, folded on the ephemeris of Table 3. **Second panel:** Binned ( $\Delta\phi = 0.0025$ ) WASP data around the transit. **Third panel:** Transit light curve obtained with Euler. **Fourth panel:** relative RV measurements of WASP-30 measured by CORALIE. **Fifth panel:** residuals about the model RV solution. **Bottom panel:** bisector spans.

TABLE 2  
EULER PHOTOMETRY OF WASP-30

BJD-2 450 000 (days)	Relative flux	$\sigma_{\text{flux}}$
5409.693659	1.00123	0.00185
5409.695116	0.99944	0.00185
5409.696482	1.00213	0.00185
...	...	...
5409.917840	1.00020	0.00185
5409.918650	0.99791	0.00185

This table is published in its entirety in the electronic edition of the *Astrophysical Journal*. A portion is shown here for guidance regarding its form and content.

diagnostics. The parameters obtained from the analysis are given in the top panel of Table 3. The elemental abundances were determined from equivalent width measurements of several clean and unblended lines. A value for microturbulence ( $\xi_t$ ) was determined from Fe I using the method of Magain (1984). The quoted error estimates include that given by the uncertainties in  $T_{\text{eff}}$ ,  $\log g_*$  and  $\xi_t$ , as well as the scatter due to measurement and atomic data uncertainties. Our quoted lithium abundance takes account of non local thermodynamic equilibrium corrections (Carlsson et al. 1994), with a value of  $A_{\text{Li}} = 2.95$  resulting when neglecting them.

The projected stellar rotation velocity ( $v \sin i$ ) was determined by fitting the profiles of several unblended Fe I lines. A value for macroturbulence ( $v_{\text{mac}}$ ) of  $4.7 \pm 0.3 \text{ km s}^{-1}$  was assumed, based on the tabulation by Gray (2008), and an instrumental FWHM of  $0.11 \pm 0.01 \text{ \AA}$ , determined from the telluric lines around  $6300 \text{ \AA}$ . A best-fitting value of  $v \sin i = 14.2 \pm 1.1 \text{ km s}^{-1}$  was obtained.

#### 4. SYSTEM PARAMETERS

The WASP and Euler photometry were combined with the CORALIE RV measurements in a simultaneous Markov-chain Monte Carlo (MCMC) analysis (Collier Cameron et al. 2007; Pollacco et al. 2008). Our proposal parameters are:  $T_c$ ,  $P$ ,  $\Delta F$ ,  $T_{14}$ ,  $b$ ,  $K_1$ ,  $T_{\text{eff}}$ ,  $[\text{Fe}/\text{H}]$ ,  $\sqrt{e} \cos \omega$  and  $\sqrt{e} \sin \omega$  (Collier Cameron et al. 2007; Enoch et al. 2010). Here  $T_c$  is the epoch of mid-transit,  $P$  is the orbital period,  $\Delta F = R_p^2/R_*^2$  is the fractional flux-deficit that would be observed during transit in the absence of limb-darkening,  $T_{14}$  is the total transit duration (from first to fourth contact),  $b$  is the impact parameter of the BD's path across the stellar disc,  $K_1$  is the semi-amplitude of the stellar reflex velocity,  $T_{\text{eff}}$  is the stellar effective temperature,  $[\text{Fe}/\text{H}]$  is the stellar metallicity,  $e$  is the orbital eccentricity and  $\omega$  is the argument of periastron.

As Ford (2006) notes, it is convenient to use  $e \cos \omega$  and  $e \sin \omega$  as MCMC jump parameters, because these two quantities are nearly orthogonal and their joint probability density function is well-behaved when the eccentricity is small and  $\omega$  is highly uncertain. Ford cautions, however, that the use of  $e \cos \omega$  and  $e \sin \omega$  as jump parameters implicitly imposes a prior on the eccentricity that increases linearly with  $e$ . Instead we use  $\sqrt{e} \cos \omega$  and  $\sqrt{e} \sin \omega$  as jump parameters, which restores a uniform prior on  $e$ .

At each step in the MCMC procedure, each proposal parameter is perturbed from its previous value by a

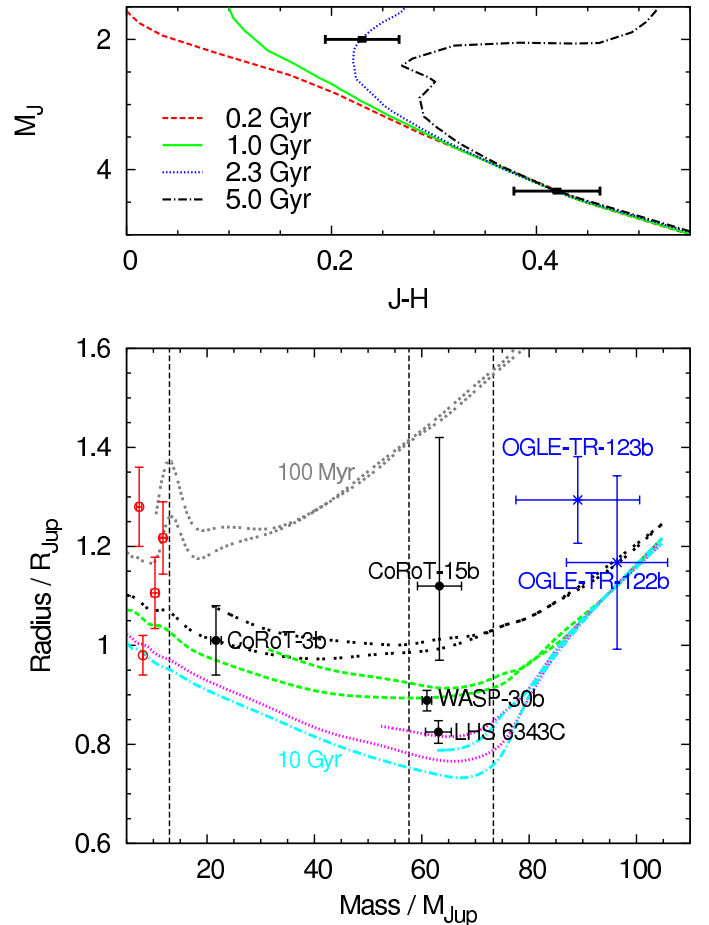


FIG. 2.— **Top panel:** Colour-magnitude diagram for WASP-30 and a nearby star with which it appears to be comoving. Isochrones for the ages shown are from Marigo et al. (2008). **Bottom panel:** Mass-radius diagram showing objects in the mass range  $5\text{--}110 M_{\text{Jup}}$  with precise radius measurements. The data are from <http://www.inscience.ch/transits/> and, in the case of LHS 6343 C, from Johnson (2010, private communication). The theoretical isochrones with ages 0.1, 0.5, 1, 5 and 10 Gyr are from the DUSTY00 and COND03 models. Those that reach down to the minimum plotted mass are the COND03 isochrones. The vertical dashed lines depict the approximate theoretical minimum masses for deuterium burning ( $13 M_{\text{Jup}}$ ), lithium burning ( $0.055 M_{\odot}$ ), and hydrogen burning ( $0.07 M_{\odot}$ ; e.g. Chabrier et al. 2000a,b).

small, random amount. From the proposal parameters, model light and RV curves are generated and  $\chi^2$  is calculated from their comparison with the data. A step is accepted if  $\chi^2$  (our merit function) is lower than for the previous step, and a step with higher  $\chi^2$  is accepted with probability  $\exp(-\Delta\chi^2/2)$ . In this way, the parameter space around the optimum solution is thoroughly explored. The value and uncertainty for each parameter are respectively taken as the median and central 68.3% confidence interval of the parameter's marginalised posterior probability distribution.

From the proposal parameters, we calculate the mass  $M$ , radius  $R$ , density  $\rho$ , and surface gravity  $\log g$  of the star (which we denote with subscript  $*$ ) and the planet (which we denote with subscript  $P$ ). At each step, the stellar density is measured from the transit light curve (Seager & Mallén-Ornelas 2003). This is input in to the empirical mass calibration of Torres et al. (2010),

as modified by Enoch et al. (2010), to obtain an estimate of the stellar mass. We also calculate the equilibrium temperature of the planet  $T_{\text{eq}}$ , assuming it to be a black-body with efficient redistribution of energy from the planet's day-side to its night-side, the transit ingress and egress durations,  $T_{12}$  and  $T_{34}$ , and the orbital semi-major axis  $a$ .

With eccentricity floating, we find  $e = 0.0021^{+0.0024}_{-0.0015}$ . Applying the 'F-test' of Lucy & Sweeney (1971), we find a 70% probability that the fitted eccentricity could have arisen by chance if the underlying orbit is in fact circular. As such, we impose a circular orbit, but we note that doing so has no significant effect on the solution in this case.

Without exquisite photometry, our implementation of MCMC tends to bias the impact parameter, and thus  $R_*$  and  $R_P$ , to higher values. This is because, with low signal-to-noise photometry, the transit ingress and egress durations are uncertain, and symmetric uncertainties in those translate into asymmetric uncertainties in  $b$  and thus on  $R_*$ . We therefore place a main sequence (MS) prior on the star, which is reasonable given the star's apparent age (Section 5). With the MS prior, a Bayesian penalty ensures that, in accepted MCMC steps, the values of stellar radius are consistent with the values of stellar mass for a main-sequence star (Collier Cameron et al. 2007).

The median parameter values and their  $1\text{-}\sigma$  uncertainties from our MCMC analysis are presented in the middle panel of Table 3. The corresponding transit light curves and RV curve are shown in Figure 1. When not imposing a MS prior, the best-fitting values we obtain are:  $b = 0.24^{+0.24}_{-0.16}$ ,  $R_* = 1.337^{+0.147}_{-0.042} R_\odot$ , and  $R_P = 0.925^{+0.118}_{-0.040} R_{\text{Jup}}$ .

## 5. SYSTEM AGE AND COMPANION RADIUS

The high lithium abundance ( $A_{\text{Li}} = 2.87 \pm 0.10$ ) found in WASP-30 implies an age most likely between that of open clusters such as  $\alpha$  Per (50 Myr;  $A_{\text{Li}} = 2.97 \pm 0.13$ ) and the Hyades (600 Myr;  $A_{\text{Li}} = 2.77 \pm 0.21$ ), and almost certainly younger than 2-Gyr-old open clusters such as NGC 752 ( $A_{\text{Li}} = 2.65 \pm 0.13$ ; Sestito & Randich 2005).

Assuming aligned stellar-spin and planetary-orbit axes, the measured  $v \sin i$  of WASP-30 and its derived stellar radius indicate a rotational period of  $P_{\text{rot}} = 4.6 \pm 0.4$  days. After removing the transits from the WASP light curves, we searched them for evidence of rotational modulation. Though there are periodogram peaks at periods of 4.1 d, 4.3 d and 4.7 d, the signal amplitudes are small. We thus conclude that there is no evidence of rotational modulation in the WASP-30 light curves, commensurate with expectations based on the star's spectral type. The 4.6 d stellar rotation period is very close to the companion's orbital period, suggesting that the two may be synchronized, thus preventing a gyrochronological age determination (Barnes 2007). The synchronization timescale (Zahn 1977) for the star is  $0.23 \pm 0.02$  Gyr.

We searched within  $15'$  of the sky position of WASP-30 for common proper motion stars. The  $V = 13.6$  star USNO-B1.0 0800-0674908 is  $13.09$  away and appears to be comoving with WASP-30 (Table 3, bottom panel). Using 2MASS photometry, we constructed a colour-magnitude diagram. A distance modulus of

TABLE 3  
SYSTEM PARAMETERS FOR WASP-30

Stellar parameters from spectroscopic analysis				
R.A. = 23 <sup>h</sup> 53 <sup>m</sup> 38.03 <sup>s</sup> , Dec. = −10°07′05.1″ (J2000)				
TYC 5834-95-1, 2MASS 23533805-1007049				
$T_{\text{eff}}$ (K)	6100 ± 100			
$\log g_*$	4.3 ± 0.1			
$\xi_t$ (km s <sup>−1</sup> )	1.1 ± 0.1			
$v \sin i$ (km s <sup>−1</sup> )	14.2 ± 1.1			
[Fe/H]	−0.08 ± 0.10			
[Si/H]	+0.04 ± 0.13			
[Ca/H]	+0.10 ± 0.14			
[Ti/H]	−0.01 ± 0.14			
[Ni/H]	−0.08 ± 0.13			
$A_{\text{Li}}$	2.87 ± 0.10			
Parameters from MCMC analysis				
$P$ (d)	4.156736 ± 0.000013			
$T_c$ (HJD)	2455334.98479 ± 0.00076			
$T_{14}$ (d)	0.1595 ± 0.0017			
$T_{12} = T_{34}$ (d)	0.01060 ± 0.00025			
$\Delta F = R_P^2/R_*^2$	0.00498 ± 0.00017			
$b$	0.066 <sup>+0.072</sup> <sub>−0.044</sub>			
$i$ (°)	89.57 <sup>+0.28</sup> <sub>−0.47</sub>			
$K_1$ (km s <sup>−1</sup> )	6.627 ± 0.015			
$a$ (AU)	0.05325 ± 0.00039			
$e$	0 (adopted)			
$\gamma$ (km s <sup>−1</sup> )	7.9177 ± 0.0099			
$M_*$ ( $M_\odot$ )	1.166 ± 0.026			
$R_*$ ( $R_\odot$ )	1.295 ± 0.019			
$\log g_*$ (cgs)	4.280 ± 0.010			
$\rho_*$ ( $\rho_\odot$ )	0.537 ± 0.019			
$T_{\text{eff}}$ (K)	6201 ± 97			
[Fe/H]	−0.03 ± 0.10			
$M_P$ ( $M_{\text{Jup}}$ )	60.96 ± 0.89			
$R_P$ ( $R_{\text{Jup}}$ )	0.889 ± 0.021			
$\log g_P$ (cgs)	5.247 ± 0.019			
$\rho_P$ ( $\rho_J$ )	86.8 ± 5.7			
$T_{\text{eq}}$ (K)	1474 ± 25			
Proper motions of WASP-30 and its neighbour				
Star	UCAC3		PPXML	
	$\mu_\alpha$ (mas/yr)	$\mu_\delta$ (mas/yr)	$\mu_\alpha$ (mas/yr)	$\mu_\delta$ (mas/yr)
WASP-30	−20.4 ± 2.2	−9.0 ± 2.4	−22.9 ± 2.2	−9.0 ± 2.4
neighbour	−23.0 ± 7.2	−8.1 ± 4.4	−18.9 ± 3.9	−9.5 ± 3.9

$8.50 \pm 0.05$  ( $500 \pm 10$  pc) was required to place the comoving star on the main-sequence and suggests that WASP-30 is  $\sim 2.3$ -Gyr old (Figure 2, upper panel). However, the apparent magnitude and spectral type of WASP-30 suggest a smaller distance modulus of  $7.9 \pm 0.2$  ( $366 \pm 77$  pc). As the comoving star may be a mere line-of-sight neighbour, this age determination should be treated with caution.

In the lower panel of Figure 2, WASP-30b is plotted in a mass-radius diagram together with isochrones of isolated BDs from models with dusty atmospheres (DUSTY00, Chabrier et al. 2000b) and models with dust-free atmospheres (COND03, Baraffe et al. 2003). By an age of 1 Gyr, an isolated BD with the mass of WASP-30b is expected to have cooled to  $T_{\text{eq}} \sim 1700$  K, and the transition from dusty L-dwarfs to dust-free T-dwarfs is expected to take place at  $T_{\text{eq}} = 1300\text{--}1700$  K (Baraffe et al. 2003). Considering this and the fact

that WASP-30b is highly irradiated, it is likely that the dusty atmosphere models of Chabrier et al. (2000b) are more representative. Depending on the transition temperature, WASP-30b may remain a dusty L-dwarf for the lifetime of its host star, or it may at some point transition to a dust-free T-dwarf.

WASP-30b has a mass of  $0.05819 \pm 0.00084 M_{\odot}$  and a radius of  $0.0914 \pm 0.0022 R_{\odot}$ . The DUSTY00 models predict the radius of an isolated,  $0.06 M_{\odot}$  BD to be 0.149, 0.104, 0.094 and  $0.084 R_{\odot}$  at ages of, respectively, 0.1, 0.5, 1 and 5 Gyr. From a simple linear interpolation of the DUSTY00 model values, the measured radius of WASP-30b and its  $1\text{-}\sigma$  uncertainty suggests its age is  $2 \pm 1$  Gyr. The measured radius is inconsistent with the DUSTY00 model for a 0.5-Gyr BD at the  $5.7\text{-}\sigma$  level and inconsistent with a 5-Gyr BD at the  $3.4\text{-}\sigma$  level, but consistent for a 1-Gyr BD at the  $1.2\text{-}\sigma$  level. This agreement would be slightly better if the DUSTY00 models took account of irradiation. Baraffe et al. (2003) find that the irradiation of a dust-free atmosphere, at the level of irradiation experienced by WASP-30b, results in radii larger by 10% for a  $1\text{-}M_{\text{Jup}}$  planet, and larger by 7% for a  $10\text{-}M_{\text{Jup}}$  planet. However, they note that the evolution of dust-free atmospheres are more affected by irradiation than are dusty atmospheres, and WASP-30b is considerably more massive.

WASP-30's lithium abundance favours a young system age of 50–600 Myr, though lithium is a poor age indicator for an F8 star, and an age of up to 2 Gyr is not ruled out. The apparent rotational synchronisation of the host star places a lower limit of 200 Myr (though the system may have been born synchronised) and a possible companion star suggests an older age of 2.3 Gyr. Given the BD's measured radius, the DUSTY00 BD model indicates an age of  $2 \pm 1$  Gyr. Taken together, we suggest that an age of 1–2 Gyr is most likely.

## 6. DISCUSSION

The discovery of WASP-30b heralds the first unambiguous observational determination of the mass-radius relation (MRR) in the BD regime, and so we have added BDs to white dwarfs and neutron stars in the list of quantum-dominated objects with radius determinations.

Chabrier & Baraffe (2000) performed the first quantitative theoretical calculation of the MRR in the substellar and low-mass star domain, predicting a minimum in

the MRR at high BD masses (see Section 3.1 of that paper). The location of WASP-30b in the MRR minimum is consistent with the quantitative prediction of Chabrier & Baraffe (2000), thus confirming the theory.

Thus far, we know of two other high-mass brown dwarfs that transit stars: CoRoT-15b ( $63 M_{\text{Jup}}$ ; Bouchy et al. 2010) and LHS 6343 C ( $63 M_{\text{Jup}}$ ; Johnson et al. 2010, Johnson 2010, private communication). The radius of CoRoT-15b ( $1.12^{+0.30}_{-0.15} R_{\text{Jup}}$ ) is uncertain and the age of the system is currently unconstrained. The faintness of the host star ( $V \sim 16$ ) makes improving this situation difficult. LHS 6343 C was found to transit one member of an M-dwarf binary system using Kepler photometry (KIC 10002261; e.g. Borucki et al. 2010). It initially seemed that LHS 6343 C was larger than predicted for a BD of its mass and age (Johnson et al. 2010). However, after a re-evaluation of the treatment of the third light in the system, it seems to be consistent (Johnson 2010, private communication).

Chabrier et al. (2000b) predict that BDs with  $M < 0.05 M_{\odot}$  do not burn lithium, those with  $M > 0.06 M_{\odot}$  burn essentially all their lithium by an age of 0.5 Gyr, and those with an intermediate mass ( $M = 0.055 M_{\odot}$ ) burn half their lithium by 0.5 Gyr, two-thirds by 1 Gyr, and three-quarters by 5 Gyr. With a mass of  $0.0582 \pm 0.0008$  and an age of 1–2 Gyr, WASP-30b is likely to have burned most of its supply of lithium.

WASP-30b has the second smallest companion-to-star size ratio ( $\Delta F = R_p^2/R_*^2 = 0.0050$ ) of all sub-stellar bodies so far discovered by ground-based transit surveys. The star in the system with the smaller size ratio, HAT-P-11 ( $V = 9.6$ ;  $\Delta F = 0.0033$ ; Bakos et al. 2010), is 8 times brighter than WASP-30. As it is far easier to find such an object around a smaller, cooler star, the discovery of WASP-30b suggests that high-mass, sub-stellar objects in short orbits around cooler stars are rare.

WASP-South is hosted by the South African Astronomical Observatory and SuperWASP-N is hosted by the Isaac Newton Group on La Palma. We are grateful for their ongoing support and assistance. Funding for WASP comes from consortium universities and from the UK's Science and Technology Facilities Council. M. Gillon acknowledges support from the Belgian Science Policy Office in the form of a Return Grant.

*Facilities:* WASP, Euler1.2m

## REFERENCES

- Alibert, Y., Mordasini, C., Benz, W., & Winisdoerffer, C. 2005, *A&A*, 434, 343
- Bakos, G. Á., et al. 2010, *ApJ*, 710, 1724
- Baraffe, I., Chabrier, G., Barman, T. S., Allard, F., & Hauschildt, P. H. 2003, *A&A*, 402, 701
- Baranne, A., et al. 1996, *A&AS*, 119, 373
- Barnes, S. A. 2007, *ApJ*, 669, 1167
- Borucki, W. J., et al. 2010, *Science*, 327, 977
- Bouchy, F., Deleuil, M., Guillot, T., Aigrain, S., Carone, L., & Cochran, W. D. 2010, *ArXiv e-prints*
- Caballero, J. A., et al. 2007, *A&A*, 470, 903
- Carlsson, M., Rutten, R. J., Bruls, J. H. M. J., & Shchukina, N. G. 1994, *A&A*, 288, 860
- Chabrier, G., & Baraffe, I. 2000, *ARA&A*, 38, 337
- Chabrier, G., Baraffe, I., Allard, F., & Hauschildt, P. 2000a, *ApJ*, 542, L119
- . 2000b, *ApJ*, 542, 464
- Collier Cameron, A., et al. 2006, *MNRAS*, 373, 799
- . 2007, *MNRAS*, 380, 1230
- Deleuil, M., et al. 2008, *A&A*, 491, 889
- Enoch, B., Collier Cameron, A., Parley, N. R., & Hebb, L. 2010, *A&A*, 516, A33+
- Ford, E. B. 2006, *ApJ*, 642, 505
- Gillon, M., et al. 2009, *A&A*, 501, 785
- Gray, D. F. 2008, *The Observation and Analysis of Stellar Photospheres*, ed. Gray, D. F.
- Hennebelle, P., & Chabrier, G. 2008, *ApJ*, 684, 395
- Irwin, J., et al. 2010, *ApJ*, 718, 1353
- Johnson, J. A., et al. 2010, *ArXiv e-prints*
- Leconte, J., Baraffe, I., Chabrier, G., Barman, T., & Levrard, B. 2009, *A&A*, 506, 385
- Lucy, L. B., & Sweeney, M. A. 1971, *AJ*, 76, 544
- Magain, P. 1984, *A&A*, 134, 189
- Marigo, P., Girardi, L., Bressan, A., Groenewegen, M. A. T., Silva, L., & Granato, G. L. 2008, *A&A*, 482, 883
- Mordasini, C., Alibert, Y., Benz, W., & Naef, D. 2008, in *Astronomical Society of the Pacific Conference Series*, Vol. 398, *Astronomical Society of the Pacific Conference Series*, ed. D. Fischer, F. A. Rasio, S. E. Thorsett, & A. Wolszczan, 235–+
- Padoan, P., & Nordlund, Å. 2004, *ApJ*, 617, 559

- Pepe, F., et al. 2005, *The Messenger*, 120, 22  
Pollacco, D., et al. 2008, *MNRAS*, 385, 1576  
Pollacco, D. L., et al. 2006, *PASP*, 118, 1407  
Queloz, D., et al. 2000, *A&A*, 354, 99  
—. 2001, *A&A*, 379, 279  
Sahlmann, J., et al. 2010, *ArXiv e-prints*  
Seager, S., & Mallén-Ornelas, G. 2003, *ApJ*, 585, 1038  
Sestito, P., & Randich, S. 2005, *A&A*, 442, 615  
Stassun, K. G., Mathieu, R. D., & Valenti, J. A. 2006, *Nature*, 440, 311  
Torres, G., Andersen, J., & Giménez, A. 2010, *A&A Rev.*, 18, 67  
Zahn, J. 1977, *A&A*, 57, 383